Influence of the interfacial roughness on electron channelling in Fe/Au(001) multilayers

2004 J. Phys.: Condens. Matter 16 1197

(http://iopscience.iop.org/0953-8984/16/8/006)

INSTITUTE OF PHYSICS PUBLISHING JOURNAL OF PHYSICS: CONDENSED MATTER

J. Phys.: Condens. Matter **16** (2004) 1197–1209 PII: S0953-8984(04)71725-7

Influence of the interfacial roughness on electron channelling in Fe/Au(001) multilayers

A Cole[1], B J Hickey[1], T P A Hase[2], J D R Buchanan[2] and B K Tanner[2]

[1] Department of Physics and Astronomy, EC Stoner Laboratory, University of Leeds, Leeds LS2 9JT, UK
[2] Department of Physics, University of Durham, Rochester Building, Science Laboratories, South Road, Durham DH1 3LE, UK

Received 11 November 2003
Published 13 February 2004
Online at stacks.iop.org/JPhysCM/16/1197 (DOI: 10.1088/0953-8984/16/8/006)

Abstract

Fe/Au(001) multilayers have been grown by molecular beam epitaxy using a new technique for the preparation of Au buffer layers on MgO(001) substrates. Scanning tunnelling microscopy and grazing incidence x-ray scattering reveal that the Au buffers have extremely low interface roughness and a long in-plane correlation length. X-ray scattering and diffraction show that multilayers grown on the new buffers, although having little difference in their crystalline structure, have much smoother interfaces than those grown on previous buffers. Compared with earlier multilayers with rougher interfaces, the giant magnetoresistance has increased by 20% due to more complete antiferromagnetic exchange coupling. Measurement of the saturation conductivity shows that the number of specular reflections occurring during electron channelling remains unchanged even though the interfacial roughness is reduced by a factor of six. It is postulated that the cause of this is either that spin-dependent scattering at the interface is being driven solely by the difference in the band structure, not by diffuse scatter at the interfaces, or that the wavelength of the transport electrons is such that the change in the roughness has no effect upon the specular scattering.

(Some figures in this article are in colour only in the electronic version)

1. Introduction

Magnetic multilayers, which consist of magnetic layers separated by non-magnetic spacers, exhibit giant magnetoresistance (GMR) and oscillatory exchange coupling, both of which have been studied extensively both theoretically and experimentally. The magnitude of the GMR and the strength of the oscillatory exchange coupling are strongly dependent on the asymmetry of the spin-dependent interface scattering [1]. The effect of the associated specular reflection on transport and coupling has been examined by a number of groups [2–4].

Fe/Au(100) has a particularly strong spin-dependent interfacial reflection probability and, in the theory of Stiles [5], which uses a Linearized augmented plane-wave implementation of the local spin-density approximation, it is predicted that the probability of reflection from Au into Fe is ∼60% larger for the minority electrons than for the majority electrons. Conversely from Fe into Au, the minority electrons are ∼20% more likely to be reflected. States are reflected back into the original material if there are no states with the same parallel momentum in the other material. While this is true for all multilayered systems, in Au/Fe(100) there is enhanced reflection asymmetry due to the presence of high minority reflection probability at points of high symmetry. At these points the s–p states couple weakly to the d states in the Fe, resulting in high reflection probabilities for minority electrons even though there are states with parallel momentum available. There is therefore a large confinement of minority electrons to the Fe and Au layers, the majority electrons passing between the two layers with a small proportion confined to the Fe layers. This, however, will only occur when the magnetic moments in adjacent Fe layers are aligned by an external magnetic field and an electron waveguide effect is then predicted [6, 7], electron channelling occurring within the Au spacer layer.

In a previous paper [8] we presented the first experimental evidence for channelling in Fe/Au multilayers. By growing epitaxial Fe/Au(001) multilayers on (001)MgO and Fe/Au(111) multilayers on *a* plane sapphire we demonstrated that much stronger channelling exists in the (001) orientation than in the (111) orientation. As the magnetization measurements showed only very weak coupling in the (111) samples and a correspondingly low GMR of 6% when compared with the (001) samples (which had a maximum GMR of 40% and antiferromagnetic coupling with ∼30% remanence), the key comparison was between the saturation conductivity of the two systems.

Using a classical free electron model the low-temperature saturation conductivity σ_{sat} for a 20-repeat system, is related to the number of specular reflections, N, at the Fe/Au interface by

$$\sigma_{\mathrm{sat}} = \frac{20\zeta N t_{\mathrm{Au}}^2}{t_{\mathrm{tot}}} + \frac{20 t_{\mathrm{Fe}}}{t_{\mathrm{tot}}}\sigma_{\mathrm{Fe}} + \sigma_{\mathrm{Buffer}} \tag{1}$$

where t_{Au} and t_{Fe} are the thicknesses of the Au and Fe layers and t_{tot} is the total multilayer thickness. ζ represents the usual constants from the Drude equation and σ_{Fe} and σ_{Buffer} are the conductivities of Fe and the buffer respectively. The phenomenological model is based on the extension of the mean free path of the electrons in the Au layers by the presence of the electron channelling, and the three terms in equation (1) represent the conductivity of a parallel array of resistors. Full justification for this equation is given in Dekadjevi [9]. Assuming that ζ was independent of the sample orientation and Au thickness, we found that the ratio of specular reflections between the two orientations $N_{(001)}/N_{(111)} = 2.7 \pm 0.1$ with $N_{(001)}$ being equal to 6.7 ± 0.1. This means that, on average, each electron scatters specularly between six and seven times before scattering diffusely [3]. (The model has been changed slightly from that of reference [8]. Although the number of reflections deduced above differs from that of reference [8], the ratio of (001) to (111) orientations remains the same.)

X-ray reflectivity measurements showed that the rms amplitude of the interfacial roughness of the (001) samples was 9.3 ± 0.2 Å whereas for the (111) samples the roughness was 3.3 ± 0.2 Å. As the (111) multilayer interfaces were of much higher quality than the (001) we concluded that the channelling was related to the symmetry of the Fermi surface rather than interface structure.

However, despite extremely careful reflection high-energy electron diffraction (RHEED) and x-ray scattering measurements, there remains a question as to whether some difference in physical properties between layers grown in the two orientations might be interfering with

the effect. This is particularly relevant to the (111) system Fe layers where a bcc to fcc phase transition occurs during layer growth [10]. As the thickness at which this phase transition occurs is comparable with the Fe thickness used, we have undertaken new experiments solely on the (001) system, where the Fe layer is deposited pseudomorphically in the bcc phase.

X-ray measurements on our earlier multilayers showed that the ratio of the correlated to uncorrelated interface roughness was 16:1, suggesting that the majority of the interfacial roughness observed in the multilayer resulted from the poor quality of the buffer layer. By using a novel growth technique to produce greatly improved Au buffer layers [11], we have grown Au/Fe(100) multilayers with significantly different interfacial properties. We find that the number of specular reflections is unchanged even though the interfacial roughness is more than halved.

2. Experimental technique

The samples were grown on a VG-80 Semicon MBE machine with a base pressure of the order of 10^{-11} Torr. MgO(001) substrates, with typical miscuts of 0.1°, were cleaned in acetone and isopropanol in an ultrasonic bath. The substrates were then annealed in ultra high vacuum (UHV) at 1100 K to remove any surface gases. RHEED measurements showed well-defined spots after annealing and then cooling to room temperature, confirming the high quality and cleanliness of the substrate. RHEED measurements were also performed *in situ* to monitor the film growth. *In situ* UHV scanning tunnelling microscopy (STM) was carried out on the top surface of the finished buffer.

Grazing incidence x-ray scattering measurements were undertaken on the XMaS beamline (BM28) at the ESRF Grenoble and at station 2.3 of the SRS at Daresbury Laboratory. Specular and diffuse data were fitted to model structures using the Bede MERCURY and Bede REFS software respectively. In the former code, a genetic algorithm is used to find the global minimum in the difference between the log absolute deviation between simulation and experiment. Standard high-resolution x-ray diffraction measurements were also undertaken on the multiaxis diffractometer at BM28 of the ESRF. The instrument could also be configured to perform in-plane surface diffraction scans. In such a geometry, the diffraction planes lie perpendicular to the film surface and the in-plane lattice parameter and mosaic spread are probed.

Magnetoresistance measurements were carried out using a four-point probe technique at 4.2 K and in fields up to 1 T. Vibrating sample magnetometry (VSM) was performed at a temperature of 30 K, chosen because impurities in the MgO single crystal substrates become superparamagnetic at temperatures below about 25 K. (Room-temperature VSM and magneto-optical Kerr effect (MOKE) measurements showed equivalent results but with a poorer signal to noise ratio.) The hysteresis loop observed at 30 K was solely the response of the Fe in the multilayer and buffer only.

3. Results

3.1. Au buffer layers

Previous multilayers were grown on Au buffers which consisted of a 10 Å Fe seed layer and a 60 Å thick Au layer. The Fe was deposited upon the MgO(001) at a rate of 0.2 Å s^{-1} and a temperature of 800 K. After cooling to 500 K the Au layer was deposited at a rate of 0.2 Å s^{-1}. This buffer is hereafter called type 1.

A topographic STM image and a line scan across typical surface features of a type 1 buffer are shown in figure 1. There are irregular, isolated islands of lateral dimensions 2–50 nm in

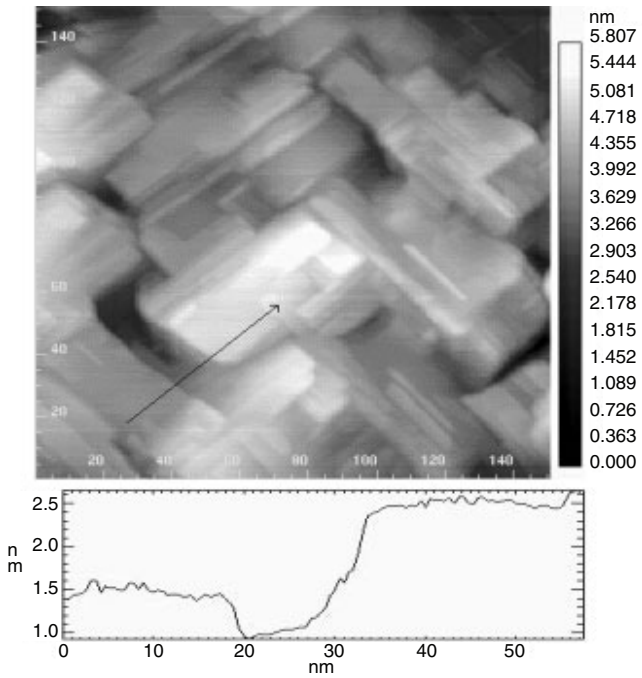

Figure 1. A typical STM picture and line scan of the buffer of the type 1 samples. RMS roughness $= 7.2 \pm 0.5$ Å.

all directions. These are separated by deep chasms, which in some places extend down to the Fe seed layer, thus proving that we do not have complete coverage.

The new buffers (type 2) were grown by a method similar to that of Spiridis *et al* [11]. The first 30 Å of Fe was deposited at 0.1 Å s^{-1} at room temperature. At this point the RHEED image consisted of large diffuse spots, indicative of transmission of the electron beam through islands. The lateral island sizes were of the order of 50 ± 10 Å [12]. As the temperature of the substrate was raised to 450 K the RHEED image changed from being purely transmissive to streaky, indicating that the in-plane correlation length of the Fe had increased [12]. After annealing for 30 min at 450 K, 300 Å of Au was deposited at a rate of 0.2 Å s^{-1}. The buffer was then further annealed for 1 h at 800 K after which the RHEED image was composed of very thin, well defined, streaks. The full-width half-height maximum (FWHM) of the streak indicated a lateral correlation length of 800 ± 100 Å. From this point the reconstruction streaks of the Au disappeared. Upon cooling to 450 K a further 3 Å of Au was deposited to enhance the subsequent layer-by-layer growth of Fe. This did not result in an appreciable change in correlation length but strong 5×5 reconstruction lines were observed in the RHEED data, indicating clean Au growth. Figure 2 shows typical topographic STM data from the top of a type 2 buffer. The surface consists of atomically flat terraces, ranging from 200 to over 1000 Å in length, which agrees favourably with the RHEED data. The steps are of monolayer height.

X-ray grazing incidence scattering measurements confirmed the dramatic drop in the amplitude of the surface roughness and the increase in the in-plane correlation length of the type 2 buffers compared with that of the type 1 systems. As shown in figure 3, the specular scatter falls very slowly with increase in scattering vector, and the visibility of the interference fringes remains high out to a remarkably large scattering angle.

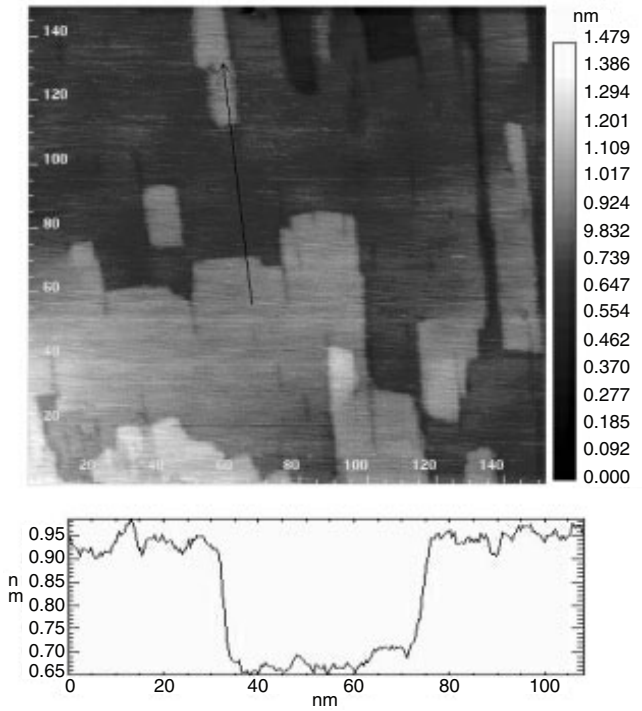

Figure 2. STM image and line scan of a type 2 buffer layer MgO(001)/Fe 30 Å/Au 303 Å. RMS roughness $= 2.0 \pm 0.5$ Å.

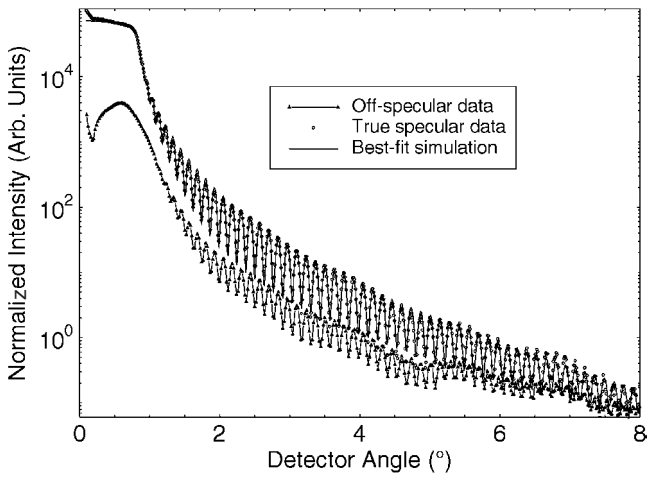

Figure 3. Specular and off-specular grazing incidence x-ray scatter from a type 2 buffer.

The Kiessig fringes in the off-specular scatter are of extremely high contrast and that contrast also remains out to a very large scattering angle. This indicates a very high level of conformity between the roughness of the substrate and the top of the buffer layer. The fit shown to the specular scatter is from a model structure in which there is a 5 Å roughness on

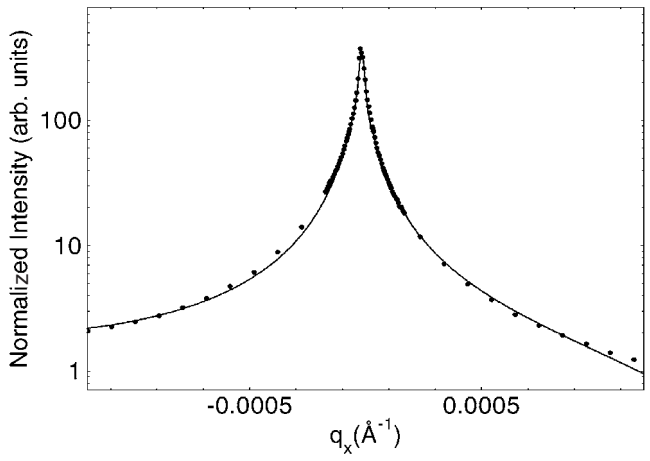

Figure 4. Transverse diffuse scatter from a type 2 buffer. The solid curve is a fit to a Lorentzian to the power 0.7.

the MgO, a 6 Å Fe buffer layer and 494 Å Au with rms roughness 1 Å. To fit the modulation a 3 Å graded oxide layer had to be included at the surface. Neither RHEED nor x-ray reflectivity measurements show any appreciable change in surface roughness over the 300–500 Å range.

Measurement of the diffuse scatter (figure 4) shows the diffuse scatter concentrated close to the specular ridge. Such a distribution is indicative of a very long in-plane correlation length, this being inversely proportional to the width of the diffuse scatter in reciprocal space. By fitting an instrument-resolved Gaussian function very close to the specular ridge, we can extract the diffuse scatter in the low-q region. The diffuse scatter (figure 4) can be fitted to a Lorentzian to the power 0.7, giving a fractal parameter h of 0.35 ± 0.05 [13]. Such a low fractal parameter is characteristic of the initial island growth of Au. The in-plane correlation length was determined from the FWHM of the fitted curve to be 5000 ± 1000 Å, consistent with the very large step lengths observed in the STM. (The precision on the correlation length is set by the difficulty of separating out the instrument resolution function. Diffuse scatter from a surface with such a long correlation length as this becomes difficult to distinguish from true specular scatter from a macroscopically tilted surface.)

3.2. Multilayers

The key question to be answered was whether the low roughness of the new buffer layers propagated through an Au/Fe multilayer. To this end we grew a range of Fe/Au(001) multilayers on type 2 buffers. The structure of the samples as grown were MgO(001)/Fe 30 Å/Au 303 Å (Fe10 Å/AuX) $\times$ 20 where the Au thickness was varied from 10–60 Å.

The specular reflectivity (figure 5) falls slowly with wavevector, with many orders of multilayer Bragg peak visible. The Kiessig fringes between the Bragg peaks arise from coherent interference between the top and bottom of the multilayer. Together these features indicate that the interface width of all layers is low. The relative multilayer Bragg peak heights and overall fall in intensity with scattering angle is matched very well by simulation and gives a best fit of 2.1 ± 0.1 Å for the Fe–Au interface width and 1.1 ± 0.1 Å for the Au–Fe interface width. This is very substantially lower than that of the multilayers grown on type 1 buffers on MgO. An Au/Fe alloy buffer layer had to be included in the simulation to obtain a good fit; we find further evidence for this and it is discussed later.

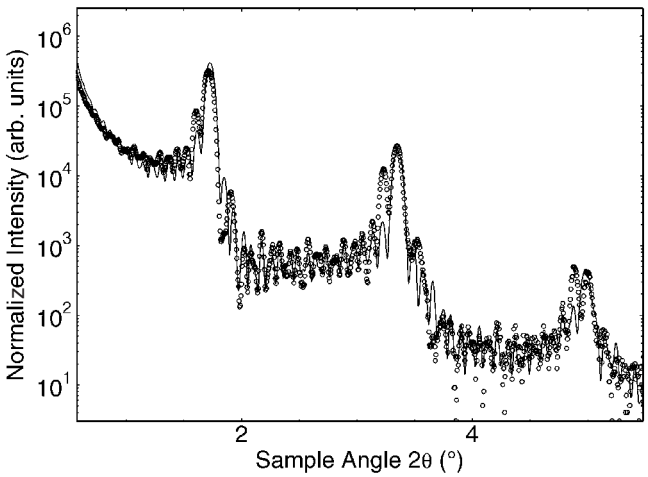

Figure 5. Specular reflectivity from a multilayer grown on a type 2 buffer.

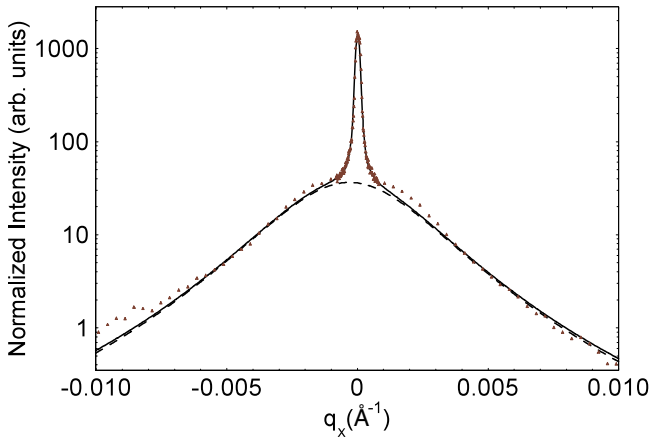

Figure 6. Transverse diffuse scan through the second multilayer Bragg peak of a multilayer grown on a type 2 buffer. The solid curve is the sum of a Lorentzian squared (dashed curve) and the instrument resolution function.

The long in-plane correlation length and the ability to reach high values of scattering vector q_z, because of the low roughness, makes the use of the Born approximation valid in analysing the diffuse scatter to extract the true topological roughness of the multilayer interfaces. The ratio of the integrated diffuse scatter I_{diff} to the integrated specular scatter I_{spec} in a transverse (rocking curve) scan through the second Bragg peak (figure 6) was 0.78, yielding an average correlated rms roughness of the multilayer interfaces of 1.6 ± 0.2 Å.

As observed previously, there is almost zero interdiffusion in the Au/Fe multilayers, the interface width measured in the specular reflection arising almost entirely from topological roughness. A good fit was found to a Lorentzian squared line shape, the full-width half-height yielding an in-plane correlation length of 510 ± 100 Å and a fractal parameter h equal to 0.75. (The uncertainty in the value of the in-plane correlation length arises primarily from the difficulty in assigning a correlation length to a line shape deduced from the Fourier transform of the fractal correlation function.)

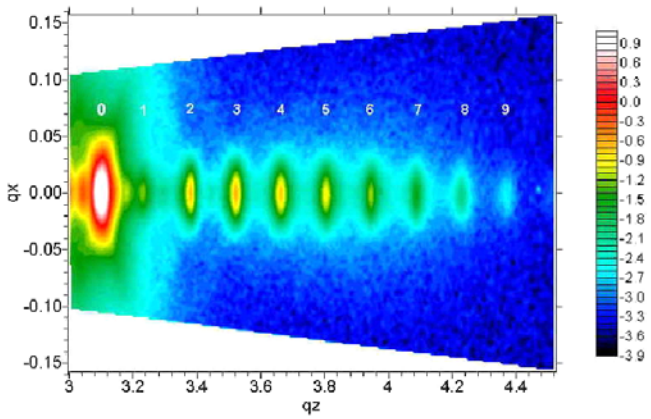

Figure 7. Full high-angle reciprocal space map around the 002 reciprocal lattice point of a multilayer on a type 2 buffer.

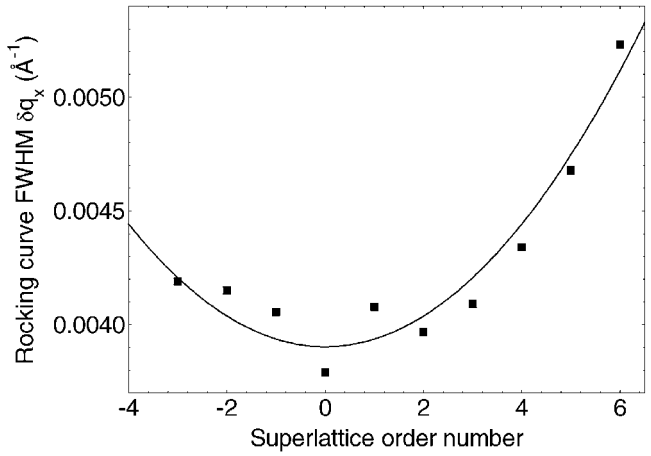

Figure 8. Rocking curve FWHM taken through successive superlattice satellite peaks around the 002 reciprocal lattice point of a multilayer on a type 2 buffer. The solid curve is a parabolic fit to the data.

Confirmation of the low multilayer interface roughness is obtained from the high-angle diffraction measurements. A full reciprocal space map around the 002 reciprocal lattice point of a sample with a Au thickness 40 Å is shown in figure 7. The high-angle high-resolution x-ray diffraction measurements are sensitive both to the long-range order within the crystal lattice itself and the structure of the artificial superlattice. There are many well-resolved superlattice satellites, out to beyond the ninth order, demonstrating very high crystal lattice perfection [14].

Rocking curves, in which the sample is scanned for fixed detector position, correspond, to a close approximation, to scans of q_x at fixed q_z. Figure 8 shows an example of the FWHM of the rocking curve as a function of satellite order. The rocking curve through the zero-order satellite is not influenced by the multilayer interface roughness, the influence of roughness resulting in an increase in the rocking curve FWHM as the square of the satellite order [15]. At the minimum in the curve of figure 8 the FWHM is determined by the out-of-plane mosaic spread and/or the lateral size of the diffracting domain. Compared with the (001) multilayers

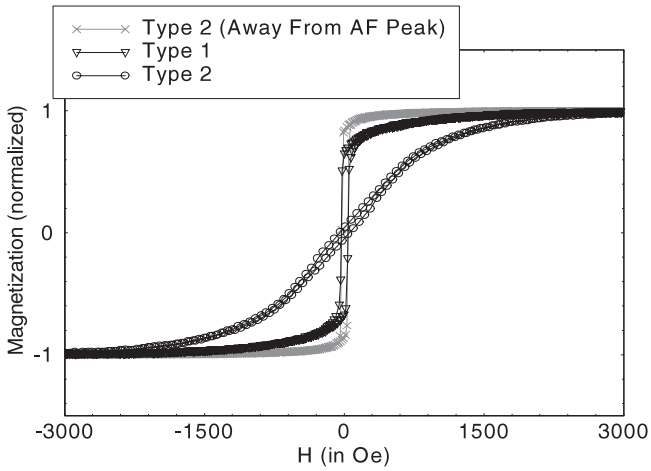

Figure 9. Typical hysteresis curve of magnetization versus field for multilayers grown at the third AF coupling peak on both buffer types. Type 2 loop away from peak (Au thickness corresponding to ferromagnetic coupling) is shown for comparison.

grown on type 1 buffers [13], the width of the zero-order satellite is an order of magnitude lower.

As in the type 1 samples a parabolic dependence with peak order is observed (figure 8), caused by the characteristic diffuse scatter from the rough interfaces adding to the mosaic scatter. However, the variation with satellite order is much weaker than for the type 1 samples, demonstrating again the lower interface roughness. The improved surface of the buffer has thus been transferred to the multilayer stack.

Hysteresis loops of multilayers grown on both buffer types show evidence of oscillatory interlayer exchange coupling. Figure 9 shows typical hysteresis loops for samples grown at the third antiferromagnetic coupling peak. In the type 2 samples the remanence is very small ($\sim 0.1 M_s$); however, the type 1 sample with the same spacer thickness shows remanence around $0.6 M_s$. The bilinear coupling constant for the type 2 sample was measured as 0.108 ± 0.004 mJ m^{-2} [16]. Even though the constant is low it compares very favourably with the results of Unguris *et al* [17] who measured the same coupling constant at this peak on a Au/Fe(001) bilayer grown on an Fe whisker. Our observation of almost the same coupling constant in a multilayer with 20 repeats again highlights the high quality of the samples in the present study. Optiz *et al* [18] and Unguris *et al* [17] suggest that extremely low levels of interfacial roughness and interdiffusion are responsible for this modest damping of the coupling constant.

GMR of multilayer samples grown on type 2 buffers (figure 10) was 20% higher than that for equivalent samples grown on type 1 buffers. The value was $58.5 \pm 0.5\%$ at 4.2 K when measured at the third antiferromagnetic coupling maximum on the type 2 buffers. (Here, the Au thickness of 18.3 Å corresponds to the third AF coupling peak observed by Unguris *et al* [17].) We note that the GMR value compares very favourably with some other reports [18] and implies that there is an anomalously low current shunting in the buffer, confining the majority of the electrons to the multilayer.

The saturation conductivity of multilayers grown on type 1 and type 2 buffers was measured along the Fe hard axis in a saturation field of 1 T at 4.2 K. Results for both are plotted in figure 11 and are fitted to equation (1). The two fit lines are almost superimposed on one another, consistent with the spread of the data points for both sample types.

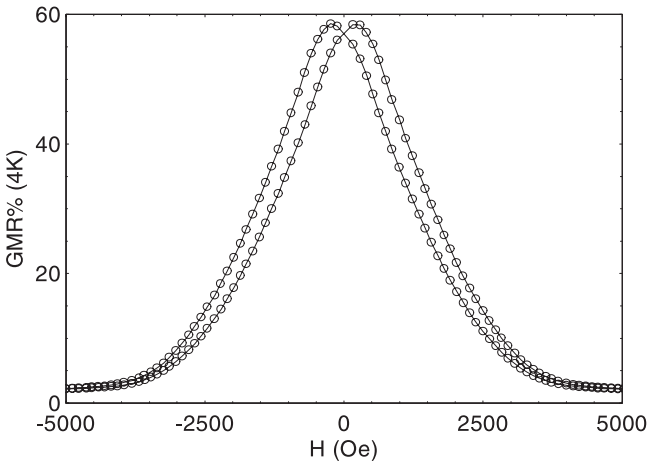

Figure 10. Magnetoresistance as a function of field on a multilayer grown on a type 2 sample (Au thickness corresponds to the third antiferromagnetic coupling peak).

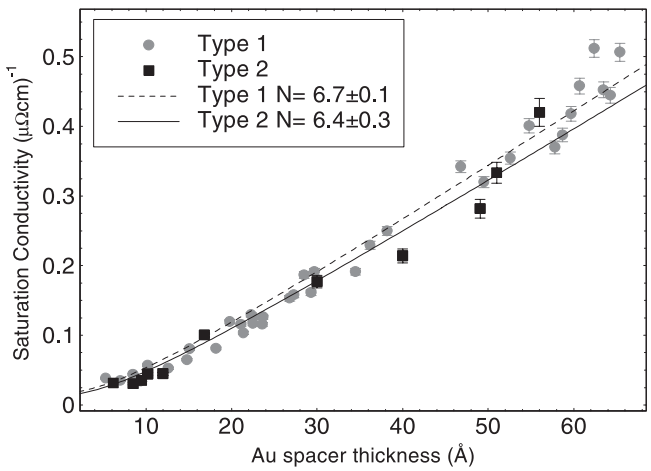

Figure 11. Saturation conductivity of multilayers grown on type 1 and type 2 buffer layers as a function of the Au layer thickness. The lines are the fits to equation (1) with N being the number of reflections for each sample type.

4. Discussion

Both the STM and the x-ray data show unequivocally that the roughness amplitude and the in-plane correlation length of Au buffers (type 2) grown by the new procedure is very substantially different from that of the original (type 1) buffer. The new buffers have a very low roughness amplitude and a long correlation length. Although this extreme smoothness is not transmitted entirely to the multilayer, the x-ray data demonstrate that the roughness is comparable with that of the (111) multilayers grown on sapphire substrates [8]. Sapphire substrates can be polished to a much lower roughness amplitude than can MgO. The low ratio of diffuse to specular scatter out to high scattering vector is indicative of low roughness. By performing the diffuse scatter measurement through the scattering vector corresponding to the scattering vector of the second multilayer Bragg peak, the dominant scatter comes from the conformal

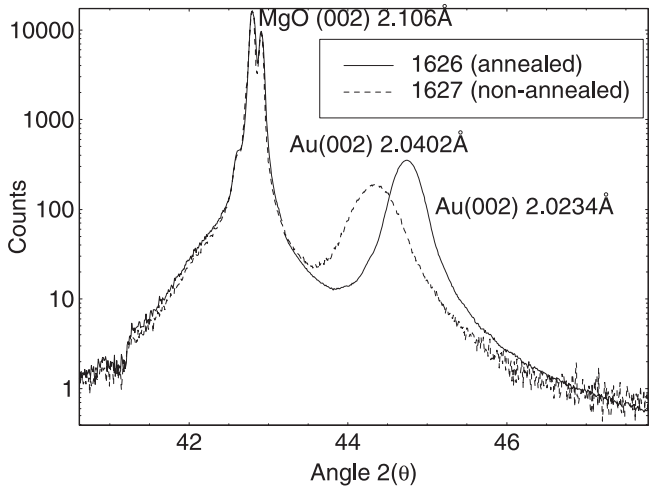

Figure 12. High-angle x-ray diffraction scans on a type 2 buffer before and after the annealing process. The data have been normalized to the MgO(002) peak.

roughness through the multilayer stack. Together with the high-angle diffraction results, the low-angle x-ray data leave us in no doubt that the (001) multilayers grown on the new buffers are half an order of magnitude smoother than multilayers grown previously.

The key result of this study is thus contained in figure 11. Despite a large reduction in the roughness amplitude and an increase in the in-plane correlation length of the multilayer interfaces, there is no significant change in the saturation conductivity. Further, there is no appreciable change in N, the number of specular reflections, the best fit to equation (1) being 6.7 ± 0.1 for type 1 buffers and 6.4 ± 0.3 for type 2 buffers. The channelling has not improved as a result of the improvement in interface perfection.

Although the type 2 buffer is a factor of five times thicker than the type 1 buffer the saturation conductivity for all Au thicknesses is almost identical for the two types of sample. Indeed, the conductivity extrapolated to zero thickness is lower for the type 2 buffer compared with the type 1. Measurement of the type 2 buffer layers shows a resistivity of $43 \pm 4\ \mu\Omega$ cm, a high value for 300 Å of Au. Further, the residual resistance ratio (RRR) of the type 2 buffer layers was close to 1, indicating that significant alloying had occurred during the annealing steps.

To test this hypothesis, x-ray diffraction measurements were carried out on the buffer before and after the annealing process. The profiles are shown in figure 12, where we note that annealing the buffer results in a shift in the position of the Au 002 peak to smaller lattice spacing, i.e. there is a reduction of the Au lattice parameter by 0.8%. The lattice parameter prior to annealing is almost identical to that of bulk Au, revealing that the Au layer is relaxed with respect to the thin Fe seed layer on the MgO. The reduction in lattice parameter cannot therefore be the result of relaxation during annealing and suggests that a dilute alloy of Fe in Au is being formed. X-ray reflectivity measurements show a shift in critical angle after annealing which could result from either a change in electron density in the Au layer or formation of a very large number of voids [19]. There is no evidence for the latter from the STM observations. Such a shift in critical angle has been seen previously during alloying of Au and Cu in Co/Cu multilayers upon annealing [20]. These observations, together with the high resistivity and low RRR, support the conclusion that a dilute alloy forms in the buffer layer during the heat treatment.

Throughout this paper we have argued that we have improved the interfaces between the Fe and Au in the multilayer but it is important to establish that the grain size and crystallographic qualities of the samples remains largely unchanged. The residual resistance ratios of the type 1 multilayer samples were 3.4 for Au thicknesses greater than 60 Å and 2.0 for Au thicknesses less than 20 Å. Equivalent type 2 multilayer samples had RRRs of 2.9 and 1.5 respectively. The similarity of these values indicates that there is no significant difference in the point defect concentration or in the interdiffusion between Fe and Au in the multilayer. Grazing incidence in-plane diffraction measurements performed on the BM28 probed the in-plane lattice perfection. Coupled '$\theta-2\theta$' in-plane scans through the 200 Bragg peak from the Au/Fe multilayer were found to have a FWHM of $0.25^\circ \pm 0.06^\circ$, unchanged between sample types [8]. As the peak width is inversely proportional to the in-plane grain size, we deduce that the grain size in the multilayer is almost identical between multilayers grown on type 1 and type 2 buffers. Hence the evidence indicates that the diffuse scattering of the electrons within the Au(001) layers is constant between the two systems and that the change is in the quality of the interfaces. We have succeeded in performing a clean experiment to test the effects of interface structure on magnetotransport without other structural changes contaminating the result.

Modifications of the interfacial quality result in no change in the number of specular reflections and hence no change in the magnitude of electron channelling in Fe/Au multilayers. Although improvement of the interfaces increases the GMR this appears to arise as a result of more complete coupling between the layers, probably by reduction in the orange peel effect. As demonstrated previously [8], the electron channelling is identified from the variation in saturation conductivity with Au thickness within the multilayer. That analysis assumed that all the scattering is taking place at the interface. The present study indicates that diffusive scattering within the Au layers, from phonons, point defects and grain boundaries, and which remains constant between both types of sample, must determine the mean free path and limit the number of specular reflections in this case to seven. To explain this effect we postulate that one or both of two effects may be occurring. One possibility is that the diffuse scattering at the magnetic/non-magnetic interface does not affect the spin-dependent scattering and such scatter, responsible for the GMR, is determined by the electronic band structure. Alternatively the wavelength of the transport electrons, which is of the order of an angstrom, is such that the five-fold decrease in the interfacial roughness does not affect the interfacial scattering probabilities, allowing the number of specular reflections to remain unchanged. To test these hypotheses we will need to grow Au/Fe multilayers with an increased in-plane grain size, keeping the interfacial roughness constant to monitor the effect of the decreasing bulk scattering which may be a factor limiting the mean free path and hence number of specular reflections. These further experiments should allow us to distinguish between the two possible mechanisms.

5. Conclusion

The most surprising result of the present study is that the electron channelling in Fe/Au multilayers is independent of the interface structure. Our structural studies of the interfaces show that an rms roughness change of a factor of six within the multilayer has no effect on the saturation conductivity. This has important implications for theoretical models of magnetotransport in these materials.

Acknowledgments

The authors wish to record their thanks to the XMaS beamline staff members, D Mannix, P Thompson, S D Brown and D F Paul for their help and assistance at the ESRF. We would

also like to thank C H Marrows for fruitful discussions. Financial support from the Engineering and Physical Science Research Council is also gratefully acknowledged.

References

[1] Stiles M D 1996 *J. Appl. Phys.* **79** 5805
[2] Enders A *et al* 2001 *J. Appl. Phys.* **89** 7110
[3] Butler W H *et al* 2000 *J. Supercond.* **13** 221
[4] Weinberger P *et al* 2003 *Phys. Rev.* B **67** 054404
[5] Stiles M D 1999 *J. Magn. Magn. Mater.* **200** 322
[6] Mathon J *et al* 1993 *J. Magn. Magn. Mater.* **121** 242
[7] Bruno P 1995 *Phys. Rev.* B **52** 411
[8] Dekadjevi D T *et al* 2001 *Phys. Rev. Lett.* **86** 5787
[9] Dekadjevi D T 2002 *PhD Thesis* University of Leeds
[10] Dekadjevi D T *et al* 2004 *Phys. Rev.* B submitted
[11] Spiridis N *et al* 1999 *Appl. Surf. Sci.* **141** 313
[12] Bourlange A *et al* 2004 at press
[13] Hase T P A *et al* 2004 at press
[14] Fulthorpe B D *et al* 2001 *J. Phys. D: Appl. Phys.* A **34** 203
[15] Holy V *et al* 1992 *Superlattices Microstruct.* **12** 25
[16] Heinrich B and Bland J A C 1994 *Ultrathin Magnetic Structures* vol 1 (Berlin: Springer)
[17] Unguris J *et al* 1997 *Phys. Rev. Lett.* **79** 2734
[18] Optiz J *et al* 2001 *Phys. Rev.* B **63** 094418
[19] Pape I *et al* 2000 *Phil. Mag.* A **80** 1913
[20] Laidler H *et al* 1996 *J. Magn. Magn. Mater.* **156** 332